CONFIDENTIAL

Copy
RM L57I24

NACA RM L57I24

RESEARCH MEMORANDUM

INVESTIGATION AT HIGH SUBSONIC SPEEDS OF THE USE OF LOW AUXILIARY TAIL SURFACES HAVING DIHEDRAL TO IMPROVE THE LONGITUDINAL AND DIRECTIONAL STABILITY OF A T-TAIL MODEL AT HIGH LIFT

By William C. Sleeman, Jr.

Langley Aeronautical Laboratory
Langley Field, Va.

NATIONAL ADVISORY COMMITTEE
FOR AERONAUTICS

WASHINGTON

December 5, 1957

CONFIDENTIAL

NACA RM L57I24 CONFIDENTIAL

NATIONAL ADVISORY COMMITTEE FOR AERONAUTICS

RESEARCH MEMORANDUM

INVESTIGATION AT HIGH SUBSONIC SPEEDS OF THE USE OF LOW AUXILIARY TAIL SURFACES HAVING DIHEDRAL TO IMPROVE THE LONGITUDINAL AND DIRECTIONAL STABILITY OF A T-TAIL MODEL AT HIGH LIFT

By William C. Sleeman, Jr.

SUMMARY

An investigation of the use of low auxiliary horizontal-tail surfaces to alleviate the pitch-up tendency at high lift of an airplane configuration having a T-tail has been conducted in the Langley high-speed 7- by 10-foot tunnel. The basic model had a wing with an aspect ratio of 3, a taper ratio of 0.143, and an unswept 80-percent chord line. The Mach number for most of the tests extended from 0.60 to 0.94 and the angle-of-attack range was from -2° to approximately 24° at the lowest test Mach number.

A preliminary study of a systematic series of auxiliary tails indicated that the pitch-up tendency at high lift encountered on the basic model could be greatly alleviated by use of a relatively small, very low-aspect-ratio auxiliary horizontal tail. This tail was located radially with respect to the fuselage center line with 30° negative dihedral and therefore provided a significant favorable increment to directional stability of the model throughout most of the test angle-of-attack range.

INTRODUCTION

The problem of the occurrence of longitudinal instability at moderate and high lift coefficients on high-speed airplane configurations has been the object of many research investigations, particularly for swept-wing arrangements. Past experience has indicated that, in general, a high tail may be used in combination with a wing of low sweep more readily than with a highly swept wing and that the pitch-up tendency

found on many wing-body arrangements can be counteracted by a horizontal tail placed below the wing chord plane. Another approach to this problem of alleviating pitch-up at high lift is the use of a biplane tail arrangement as demonstrated in the results of references 1 and 2. This type of tail configuration was designed to operate on the principle that the low tail enters or remains in a more favorable downwash field as the high tail approaches the large downwash gradients in the wing wake at high angles of attack. Thus the unfavorable contribution of the high tail is counteracted by the stabilizing contribution of the low tail.

Many current high-speed airplane configurations also have been found to be deficient in directional stability at moderate and high angles of attack and many modifications and devices have been studied in attempts to minimize this reduction in stability with angle of attack. The experimental results of reference 3 have shown that significant improvements in high-angle-of-attack directional stability could be achieved for a swept-wing model by use of very low-aspect-ratio ventral fins located radially 45° below the fuselage center line. These test results suggested the possibility that improvements in directional stability at high angles of attack as well as at 0° could be realized by using negative dihedral in the low auxiliary horizontal tail selected to improve the longitudinal characteristics at high lift.

The present investigation was conducted on a general research model having an aspect-ratio-3 wing with an unswept 80-percent chord line and a taper ratio of 0.143. The horizontal tail had a 45° delta plan form and was mounted at the tip of a moderately swept vertical tail approximately 73 percent of the wing semispan above the wing chord plane. The auxiliary tail that was tested most extensively had an exposed panel aspect ratio of 0.28 and was located approximately 16 percent of the wing semispan below the wing chord plane and had -30° dihedral. The test Mach number range extended from 0.60 to 0.94 for most of the tests and the maximum angle-of-attack range covered was from approximately -2° to 24° at the lowest test Mach number.

SYMBOLS

The lateral stability results of this investigation are referred to the body-axis system shown in figure 1 together with an indication of positive directions of forces, moments, and displacements of the model. The lift and drag characteristics presented are respectively normal to and parallel with the relative wind as shown in the side view of the model in figure 1. Moment coefficients are given about the reference center shown in figure 2 except where indicated otherwise.

C_L lift coefficient, $\frac{\text{Lift}}{qS}$

C_D drag coefficient, $\frac{\text{Drag}}{qS}$

C_m pitching-moment coefficient, $\frac{\text{Pitching moment}}{qS\bar{c}}$

C_l rolling-moment coefficient, $\frac{\text{Rolling moment}}{qSb}$

C_n yawing-moment coefficient, $\frac{\text{Yawing moment}}{qSb}$

C_Y lateral-force coefficient, $\frac{\text{Lateral force}}{qS}$

b wing span, 2.281 ft

$\bar{c}$ wing mean aerodynamic chord, 0.903 ft

S wing area, 1.74 sq ft

M Mach number

q dynamic pressure, lb/sq ft

i_t stabilizer incidence of basic horizontal tail, positive trailing edge down, deg

α angle of attack of fuselage center line, deg

β angle of sideslip, deg

Subscripts:

β denotes partial derivative of a coefficient with respect to sideslip, for example, $C_{n_\beta} = \frac{\partial C_n}{\partial \beta}$

t denotes increment in a coefficient resulting from addition of tail surfaces

Configuration designation:

W	wing
F	fuselage
V	vertical tail
H	basic horizontal tail
T_3	auxiliary tail 3

MODEL DESCRIPTION

The basic model configuration used in this investigation is shown in figure 2 with auxiliary tail 3 in place on the fuselage. Tabulated geometric characteristics of the model are given in table I. The steel wing of the model had an aspect ratio of 3, a taper ratio of 0.143, and an unswept 80-percent chord line (28.82° sweep of quarter chord). The streamwise airfoil section of the wing was NACA 65A004. The vertical tail had 28° sweepback of the quarter chord and had NACA 65A006 airfoil sections streamwise and the 45° delta-plan-form horizontal tail also had NACA 65A006 airfoil sections. The various auxiliary tail plan forms studied in the preliminary evaluation are shown in figure 2. These tails were constructed of 1/16-inch-thick brass and had rounded leading edges and blunt trailing edges. The largest tail (tail 1) was tested on the model and then the span of this tail was reduced in 1-inch increments to obtain tail 2 and tail 3. Tail 4 was formed by removing the area forward of a line on tail 3 connecting the root leading edge and tip trailing edge. All the auxiliary tails were located radially with respect to the fuselage center line with -30° dihedral.

TESTS AND CORRECTIONS

Tests

The present investigation was conducted in the Langley high-speed 7- by 10-foot tunnel over a Mach number range from 0.60 to 0.94 for the basic model and with auxiliary tail 3. The test Reynolds number based on the wing mean aerodynamic chord varied from approximately 2.6×10^6 to 3.4×10^6 from the lowest to highest test Mach number. Selection of an auxiliary tail size was made on the basis of tests of each of the low tails at $M = 0.60$; therefore, experimental results for tails 1, 2,

and 4 were obtained only at this Mach number. The maximum angle-of-attack range covered in the present investigation was from approximately -2° to 24° at the lowest Mach number. At the highest Mach numbers the angle-of-attack range was limited by aerodynamic loads on the model.

The model was mounted on a six-component strain-gage balance which was supported by a variable angle sting. The longitudinal stability characteristics were obtained from tests through the angle-of-attack range at 0° sideslip and the lateral stability derivatives were obtained from tests through the angle-of-attack range at fixed sideslip angles of $\pm 4^{\circ}$.

Corrections

Jet-boundary corrections to the angles of attack and drag coefficients determined from reference 4 were added to the data. Blockage corrections applied to the data were determined from reference 5. Drag coefficients have been corrected for a tunnel buoyancy effect and corrections have been applied such that the base-pressure conditions correspond to free-stream static-pressure conditions.

The model angles of attack and sideslip have been corrected for deflection of the balance and sting support under load.

RESULTS AND DISCUSSION

Presentation of Results

Longitudinal stability characteristics of the basic model (T-tail) for a stabilizer incidence of -1.4° and of the model with each of the auxiliary low tails are given in figure 3 for a Mach number of 0.60. Longitudinal stability characteristics for the tail-off configuration, the basic T-tail configuration with a stabilizer incidence of -7.9°, and the model with auxiliary tail 3 are given in figure 4 for the test Mach number range. Lateral stability derivatives for these configurations are given in figure 5. Figure 6 presents the pitching-moment characteristics of the basic model and the model with the different auxiliary tails having the moment reference transferred so that all the configurations had approximately the same low-lift static margin as the basic model. The tail contribution to pitching moments and directional stability is summarized in figure 7 for 0.60 Mach number.

Discussion

Effect of auxiliary tail size on pitching moments.- The test results presented in figure 3 show that increases in stability occurred with increasing size of the auxiliary tails over the entire lift range. These results have been recomputed on the basis of maintaining a given value of longitudinal stability at low lift in order to make a more rational comparison of effects of auxiliary tail size at high lift where pitch-up was indicated for the basic model. The results presented in figure 6 were obtained from figure 3 with all configurations given approximately the same low-lift stability as the basic high-tail model. The pitching-moment curves of figure 6 show that the abrupt and extensive pitch-up tendency evident for the basic model could be alleviated and delayed to a higher angle of attack by addition of the auxiliary tails. The benefits of the auxiliary tail were roughly proportional to tail size and the pitch-up tendency was almost eliminated by use of the largest auxiliary tail. In addition to the benefits of the auxiliary tails in providing negative pitching-moment increments at the highest angles of attack (C_L greater than 0.80) a significant beneficial effect also existed at lower angles. This benefit was characterized by a rather extensive increase of stability with the auxiliary tails on over the angle-of-attack range from about 10° to 18°. This increase of stability with increasing lift coefficient would be expected to make the pitch-up region more difficult to enter for an airplane having these characteristics in comparison to an arrangement showing decreasing stability just prior to the point of reversal in the pitching-moment curve.

The effects of auxiliary tail size for a constant low-lift stability just discussed were based on stability adjustment by varying the moment reference location for the bi-tail arrangements. Another, perhaps more practical, means for maintaining a given low-lift stability would be to keep the moment center fixed and reduce the area of the T-tail to compensate for the stability contributed at low lift by the auxiliary tail. This type of adjustment, when compared with the basic model, would provide a benefit not shown in the preceding analysis in that reduction in the size of the T-tail would be expected to reduce its contribution to the high-angle-of-attack instability. Such an arrangement would probably show a smaller pitch-up tendency at high lift when compared with the results given in figure 6 with the auxiliary tail on.

Longitudinal stability with auxiliary tail 3.- The largest auxiliary tails showed the greatest benefits in increasing longitudinal stability; however, it may be desirable to minimize the auxiliary tail area from other considerations. Tail 3 was therefore selected as an arrangement which afforded significant pitching-moment gains and was of small enough size not to affect adversely the maximum landing attitude by projecting below the fuselage. Test data obtained through the Mach number range

with tail 3 are presented in figure 4 with results for the basic model and for tail off. The tail-on results of figure 4 were obtained with the high horizontal tail set at an incidence angle of -7.9° rather than at -1.4° as in figure 3. This negative setting was selected to trim the model at the higher angles of attack in order to reduce the chance of interpreting tail stall as pitch-up. The pitching-moment results of figure 4 show the same trends with angle of attack and the same incremental effects from addition of auxiliary tail 3 as shown for the -1.4° stabilizer setting presented in figure 3.

The tail contribution to pitching moments with and without the auxiliary tail were determined from the data of figure 4 and are presented in figure 7 which also shows the incremental contribution of the auxiliary tail. The results summarized in figure 7 show a substantial reduction in the nose-up moments at high angles of attack when the auxiliary tail was used. In addition, the stability contribution remained relatively unchanged with increasing angle of attack up to approximately 16° where it began to increase with the auxiliary tail.

Lateral stability derivatives with auxiliary tail 3.- Lateral stability derivatives showing effects of addition of the tail surfaces to the wing-body configuration and effects of adding auxiliary tail 3 to the basic model are given in figure 5. These results show that the auxiliary tail increased the overall directional stability of the basic model at 0° angle of attack about 20 percent. Increases in directional stability were contributed by the auxiliary tail over the test angle-of-attack range; however, the magnitude of the contribution varied at the higher angles of attack. The contributions of the vertical tail and the auxiliary horizontal tail to directional stability are given in figure 7 to show more clearly the variation of the individual contributions with angle of attack. The results of figure 7 show the occurrence of significant losses in tail contribution for angles of attack above approximately 15° for both the vertical tail and the auxiliary tail. The losses in vertical-tail contribution at high angles were to be expected on the basis of past experience; however, the losses shown for the auxiliary tail would not be expected to arise from the same source as for the vertical tail.

Some discussion of the wing-fuselage characteristics may be enlightening with regard to the losses in directional stability contribution of the auxiliary tail at high angles of attack. The wing-fuselage directional stability results (fig. 5) show the large increase in instability in changing from low to moderately high angles of attack which is frequently found on highly swept, midwing-body arrangements. Reference 6 presents results which show that this increase in directional instability was associated with adverse wing-fuselage flow interference on the afterbody. This increase of instability which did not occur for the body

alone could be essentially eliminated by removal of the afterbody or could be accentuated by changing from a tapered to a cylindrical afterbody as indicated in reference 6 for a swept-wing arrangement. Inasmuch as the wing-interference effects on the afterbody appeared to be very large for the present model, the possibility exists that the favorable low angle-of-attack benefits of the auxiliary tail could diminish appreciably or perhaps become adverse at the higher angles of attack. No adverse effects of the auxiliary tail on directional stability were shown; however, the trends with angle of attack shown in the tail-off C_{n_β} curve (fig. 5) was the same as those shown for the contribution of the auxiliary tail (fig. 7). These similar trends suggest that the auxiliary tail may have been influenced by the same interference which caused the wing-fuselage instability to vary with angle of attack.

SUMMARY OF RESULTS

An investigation of the use of a low-auxiliary horizontal tail to alleviate the pitch-up tendency at high lift encountered on an airplane configuration having a high tail revealed the following results:

1. The pitch-up tendency encountered on the basic model could be alleviated by use of a relatively small low-aspect-ratio auxiliary tail placed low on the model afterbody.

2. In addition to the sizable negative pitching-moment increments obtained with the auxiliary tail above the angle of attack at which the basic model became unstable, the model showed increasing stability with increasing lift coefficient up to the angle for pitch-up for the complete model with the auxiliary tail.

3. The auxiliary tail which had -30° dihedral provided substantial increments to directional stability at low angles of attack and at the highest angles tested; however, at moderately high angles the benefits were somewhat reduced.

Langley Aeronautical Laboratory,
National Advisory Committee for Aeronautics,
Langley Field, Va., September 11, 1957.

REFERENCES

1. Few, Albert G., Jr.: Investigation at High Subsonic Speeds of the Static Longitudinal Stability Characteristics of a Model Having Cropped-Delta and Unswept Wing Plan Forms and Several Tail Configurations. NACA RM L55I23a, 1955.

2. Goodson, Kenneth W.: Static Longitudinal Characteristics at High Subsonic Speeds of a Complete Airplane Model With a Highly Tapered Wing Having the 0.80 Chord Line Unswept and With Several Tail Configurations. NACA RM L56J03, 1957.

3. Spearman, M. Leroy, Robinson, Ross B., and Driver, Cornelius: The Effects of the Addition of Small Fuselage-Mounted Fins on the Static Directional Stability Characteristics of a Model of a 45° Swept-Wing Airplane at Angles of Attack Up to 15.3° at a Mach Number of 2.01. NACA RM L56D16a, 1956.

4. Gillis, Clarence L., Polhamus, Edward C., and Gray, Joseph L., Jr.: Charts for Determining Jet-Boundary Corrections for Complete Models in 7- by 10-Foot Closed Rectangular Wind Tunnels. NACA WR L-123, 1945. (Formerly NACA ARR L5G31.)

5. Herriot, John G.: Blockage Corrections for Three-Dimensional-Flow Closed-Throat Wind Tunnels, With Consideration of the Effect of Compressibility. NACA Rep. 995, 1950. (Supersedes NACA RM A7B28.)

6. Polhamus, Edward C., and Spreeman, Kenneth P.: Subsonic Wind-Tunnel Investigation of the Effect of Fuselage Afterbody on Directional Stability of Wing-Fuselage Combinations at High Angles of Attack. NACA TN 3896, 1956.

TABLE I.- GEOMETRIC CHARACTERISTICS OF MODEL

Wing:	
Area, sq ft	1.74
Aspect ratio	3
Taper ratio	0.143
Sweep of quarter chord, deg	28.82
Mean aerodynamic chord, ft	0.903
Vertical tail:	
Exposed area, sq ft	0.406
Exposed aspect ratio	0.972
Taper ratio	0.481
Sweep of quarter chord, deg	28.00
Mean aerodynamic chord, ft	0.673
Horizontal tail:	
Area, sq ft	0.337
Aspect ratio	4
Taper ratio	0
Sweep of quarter chord, deg	36.85
Mean aerodynamic chord, ft	0.388
Auxiliary tails:	
Exposed area, sq ft:	
Tail 1	0.306
Tail 2	0.267
Tail 3	0.201
Tail 4	0.125

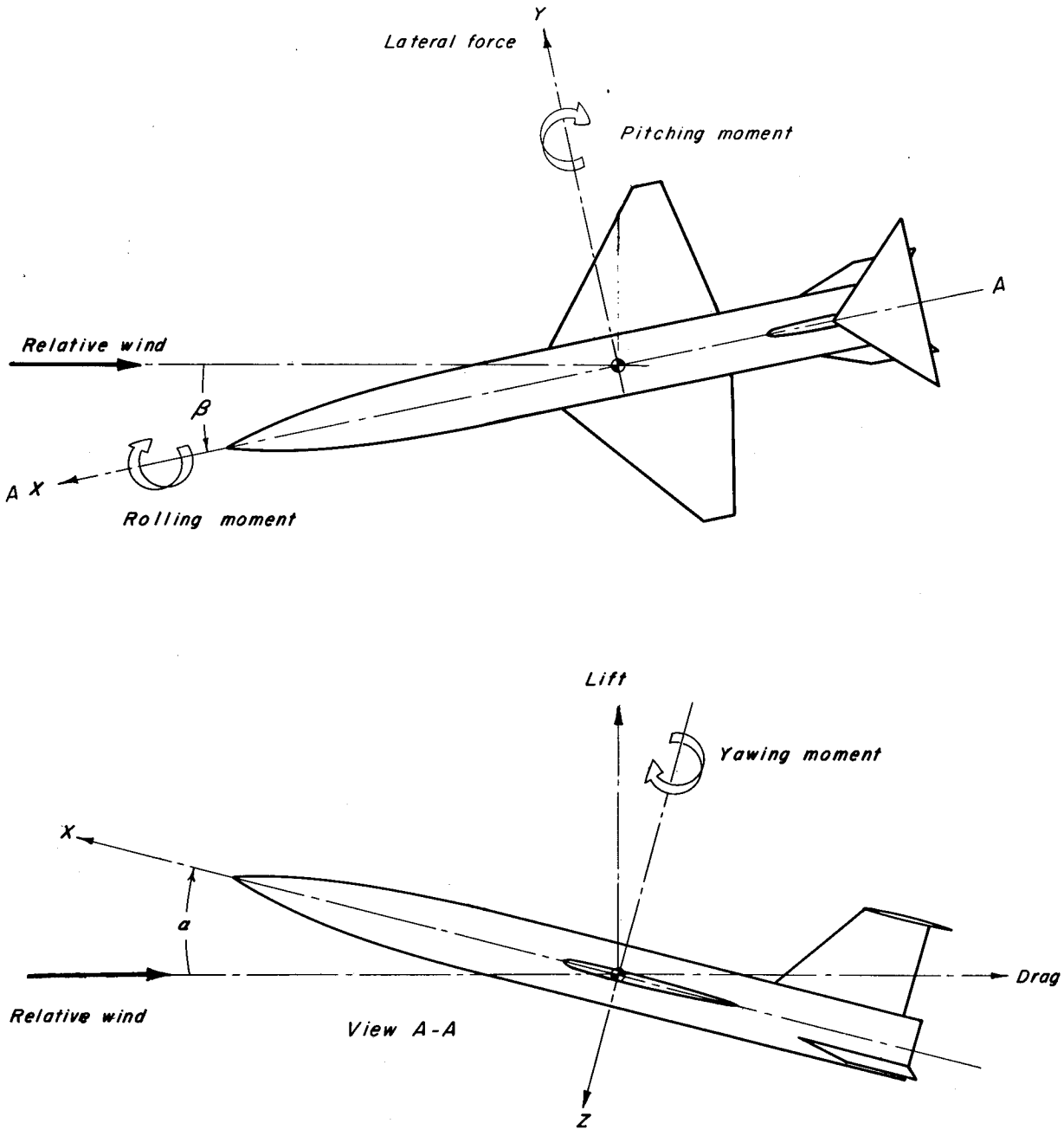

Figure 1.- Reference axes showing positive directions of forces, moments, and angular deflections.

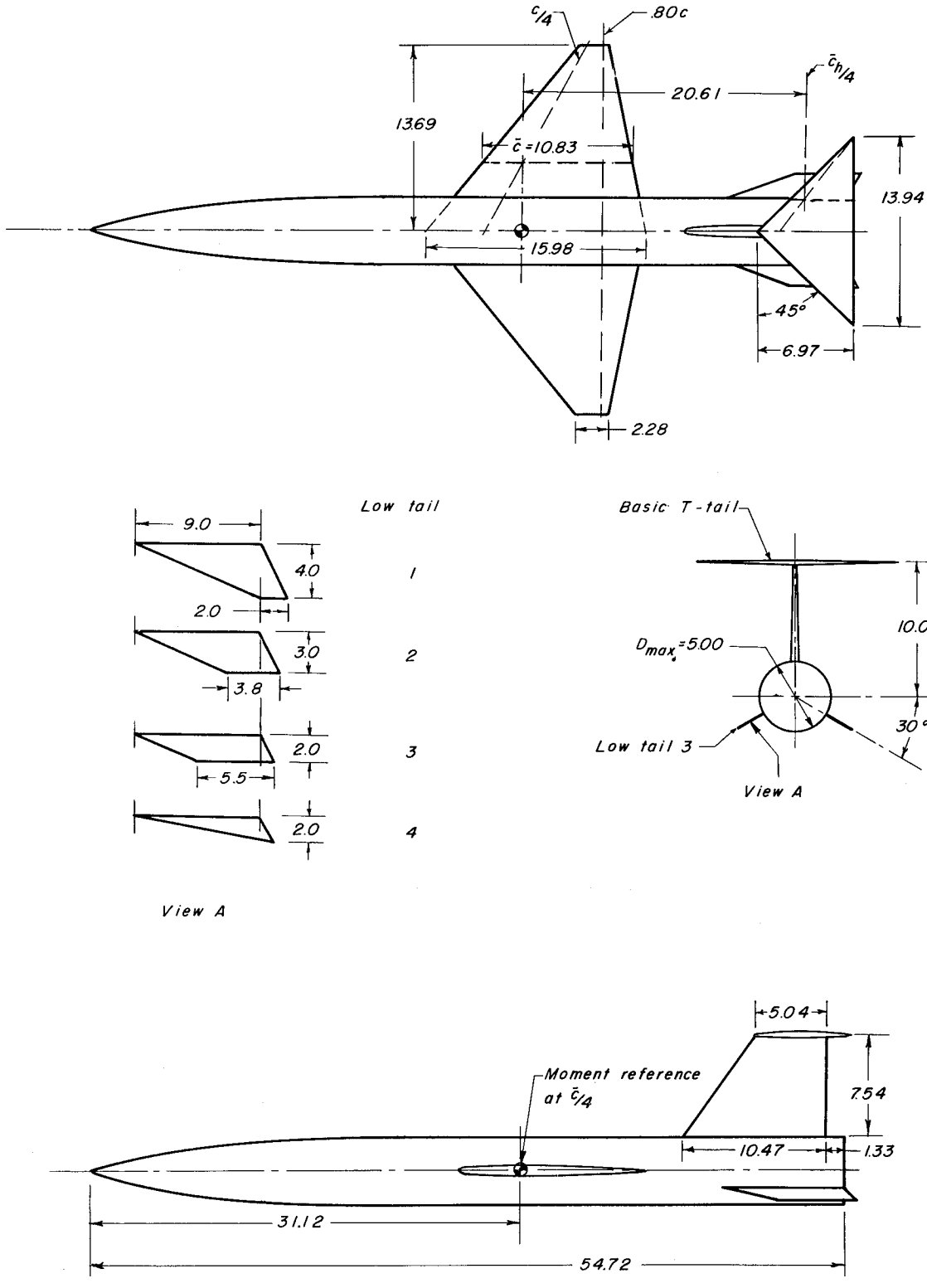

Figure 2.- General arrangement of the model used in the present tests showing details of the various auxiliary tail sizes studied.

Figure 3.- Effect of auxiliary tail size on the aerodynamic characteristics in pitch of the model at M = 0.60. i_t = -1.4°.

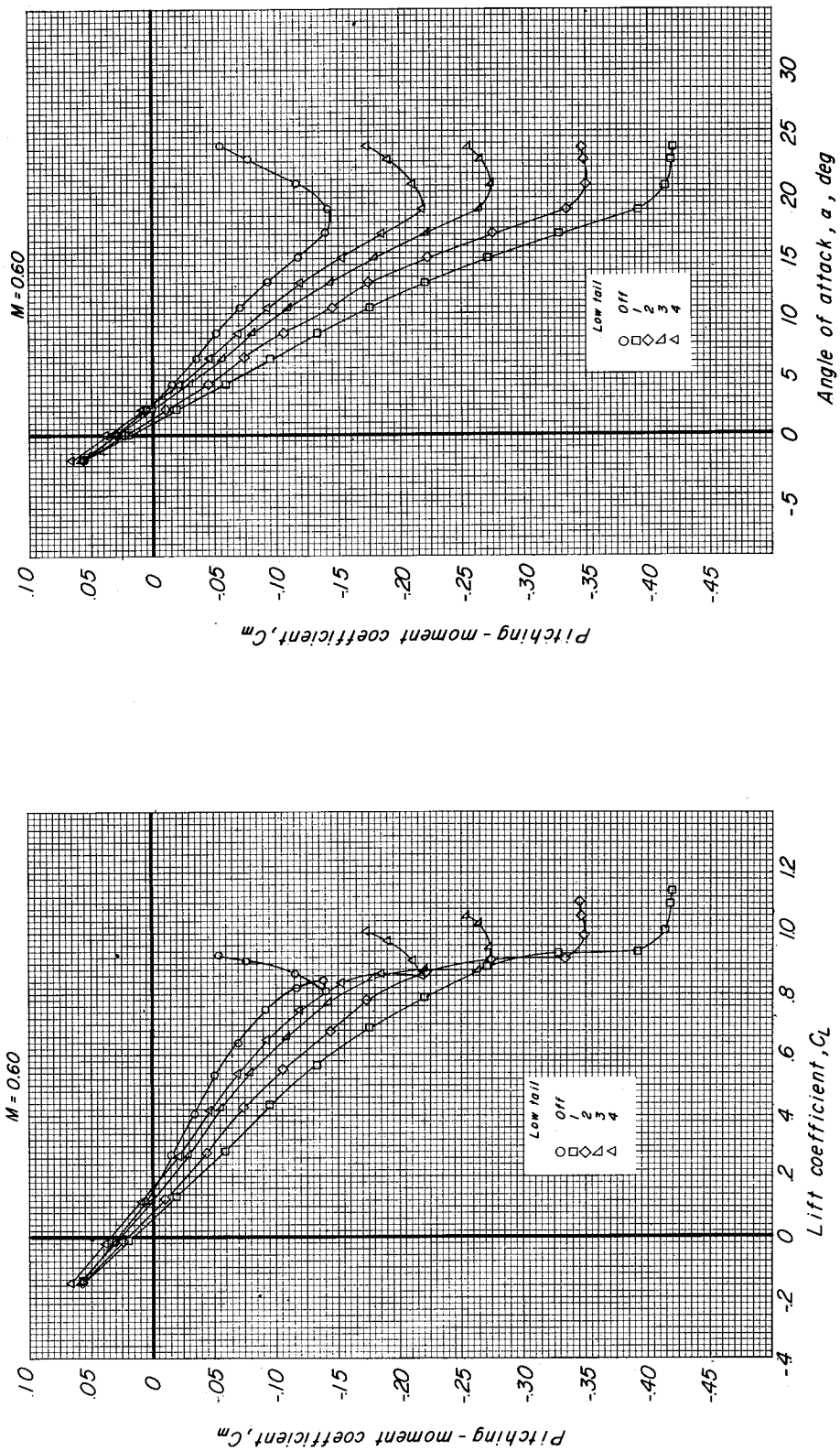

Figure 3.- Concluded.

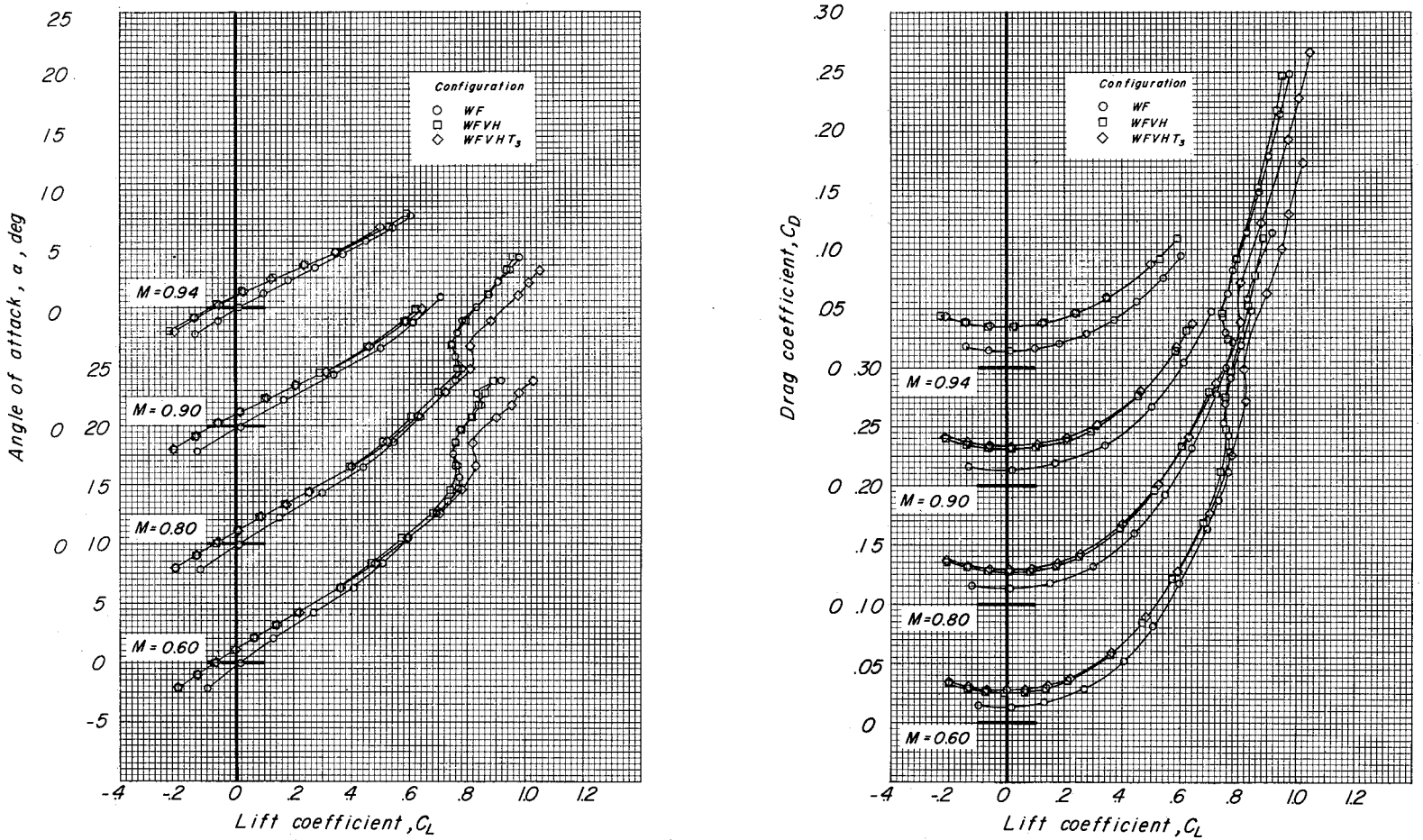

Figure 4.- Effects of addition of the basic tail surfaces and addition of auxiliary tail 3 on the longitudinal characteristics through the test Mach number range. $i_t = -7.9^\circ$.

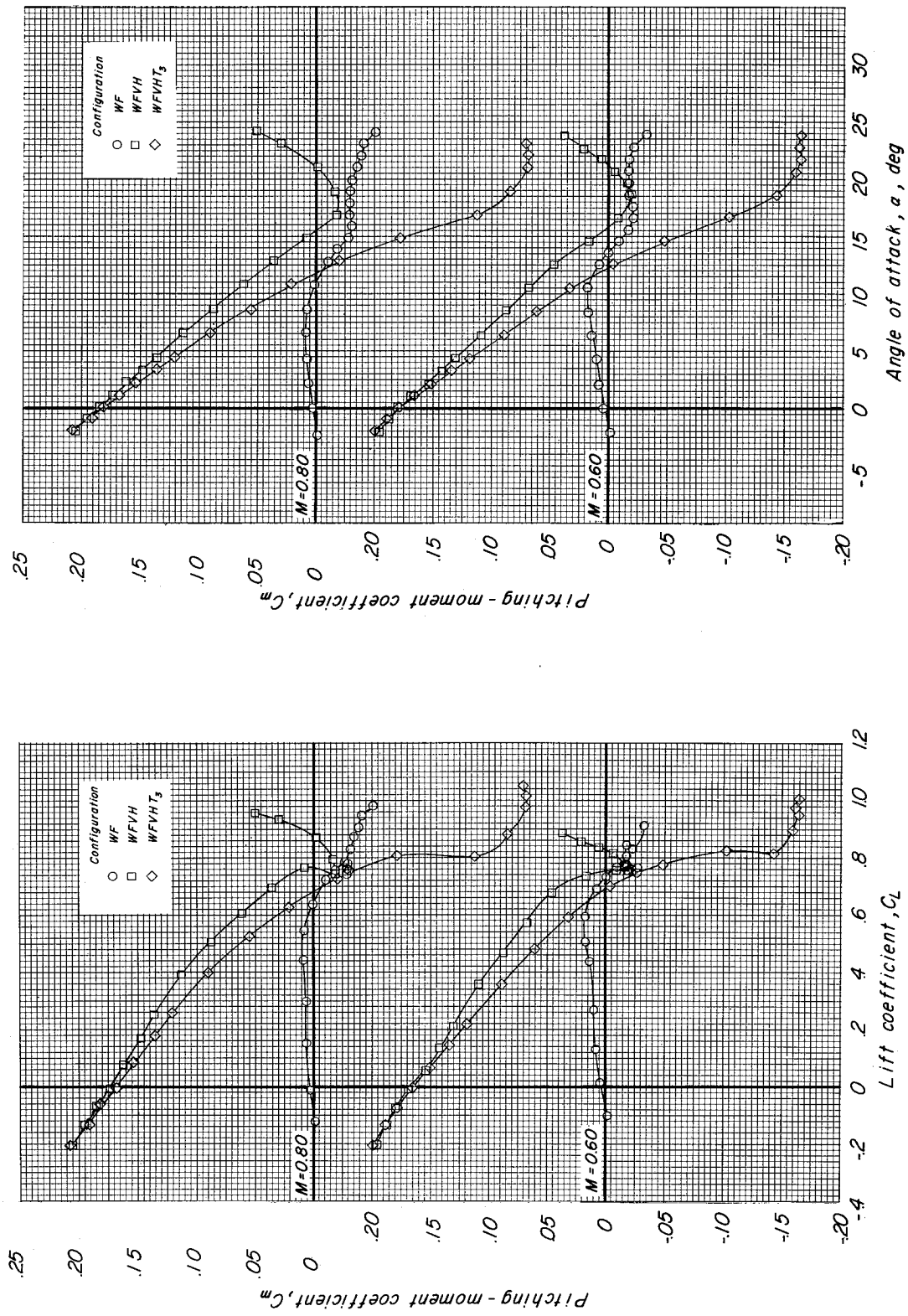

Figure 4.- Continued.

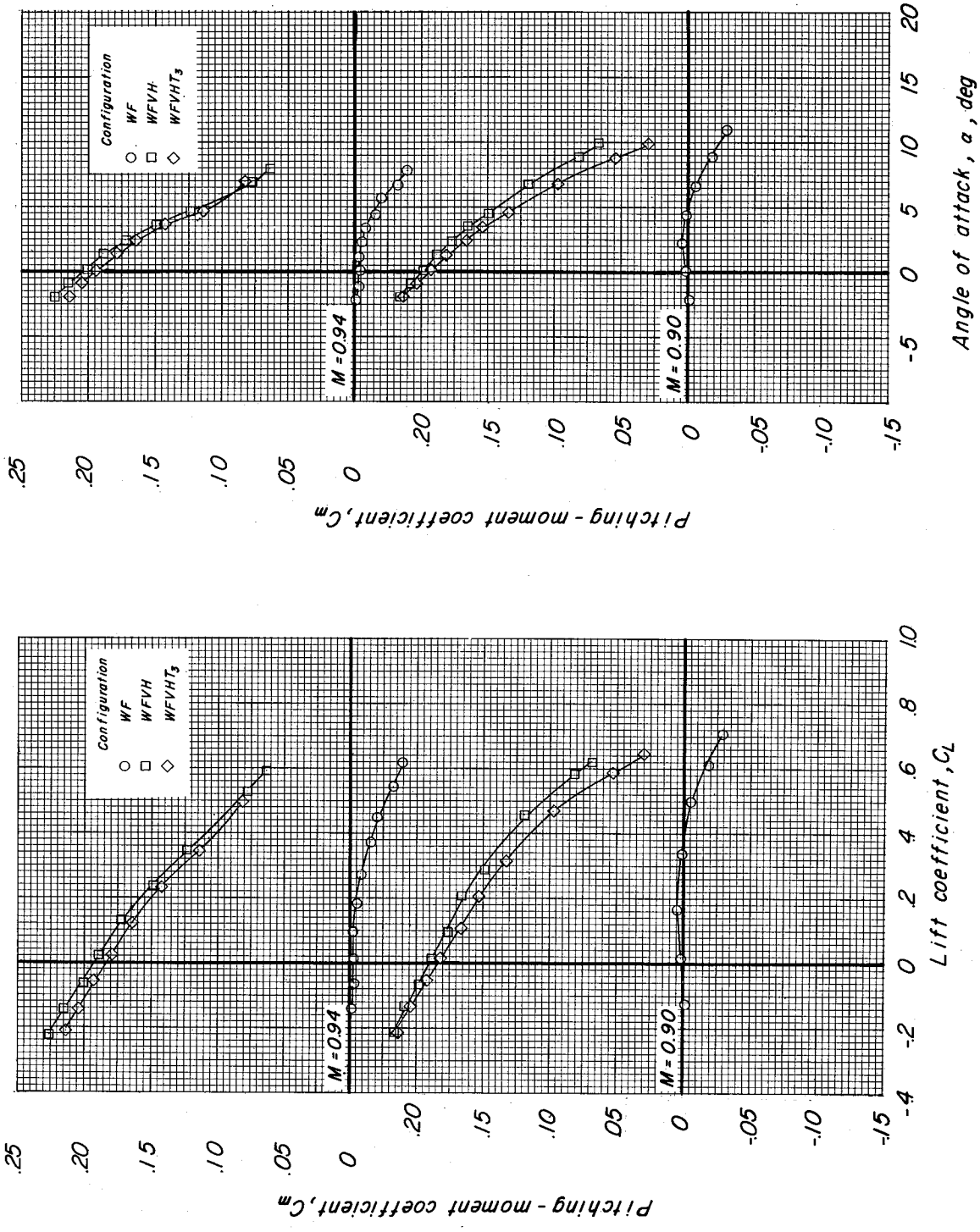

Figure 4.- Concluded.

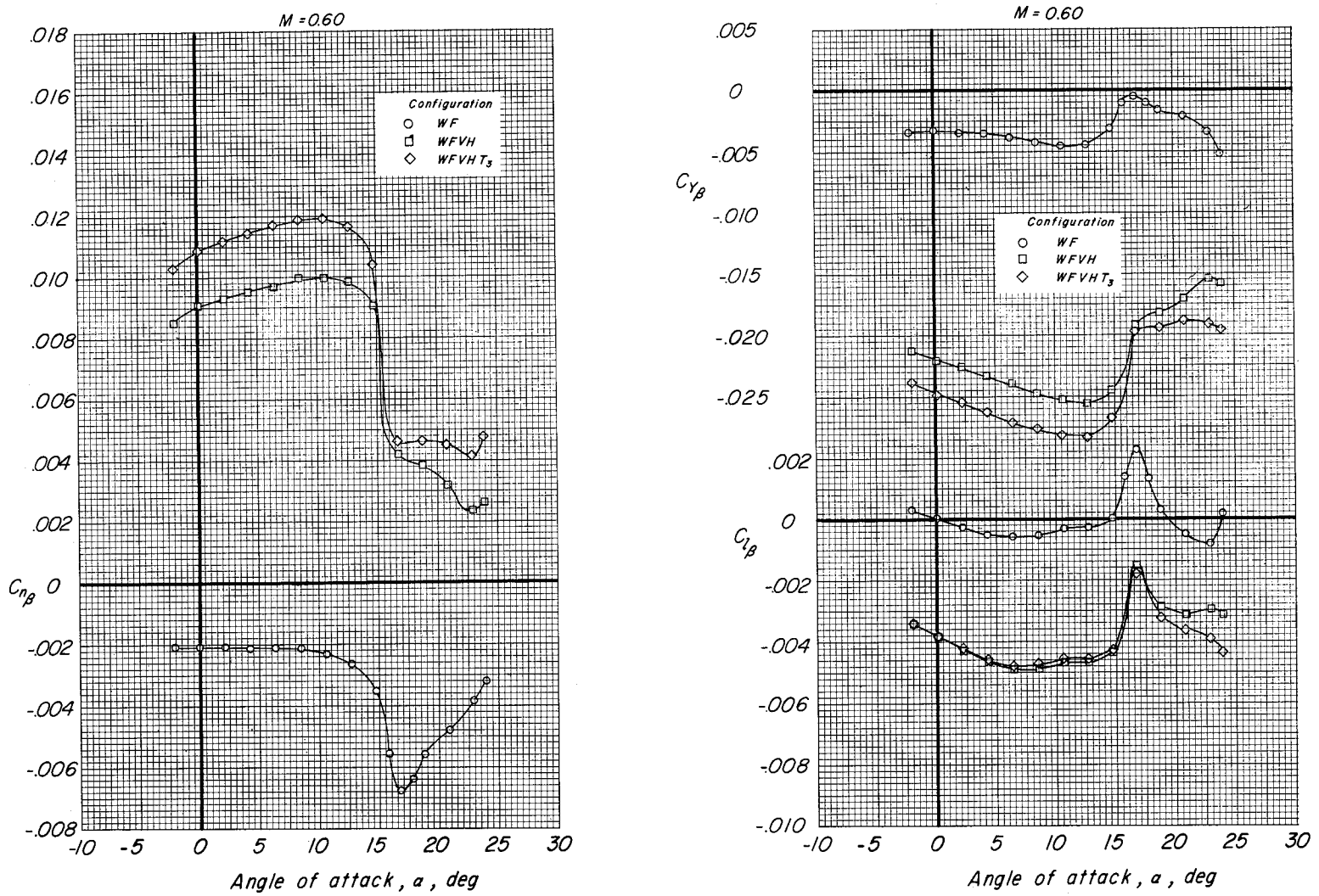

Figure 5.- Effect of addition of the basic tail surfaces and addition of auxiliary tail 3 on the lateral stability characteristics of the model through the test Mach number range. $i_t = -7.9^\circ$.

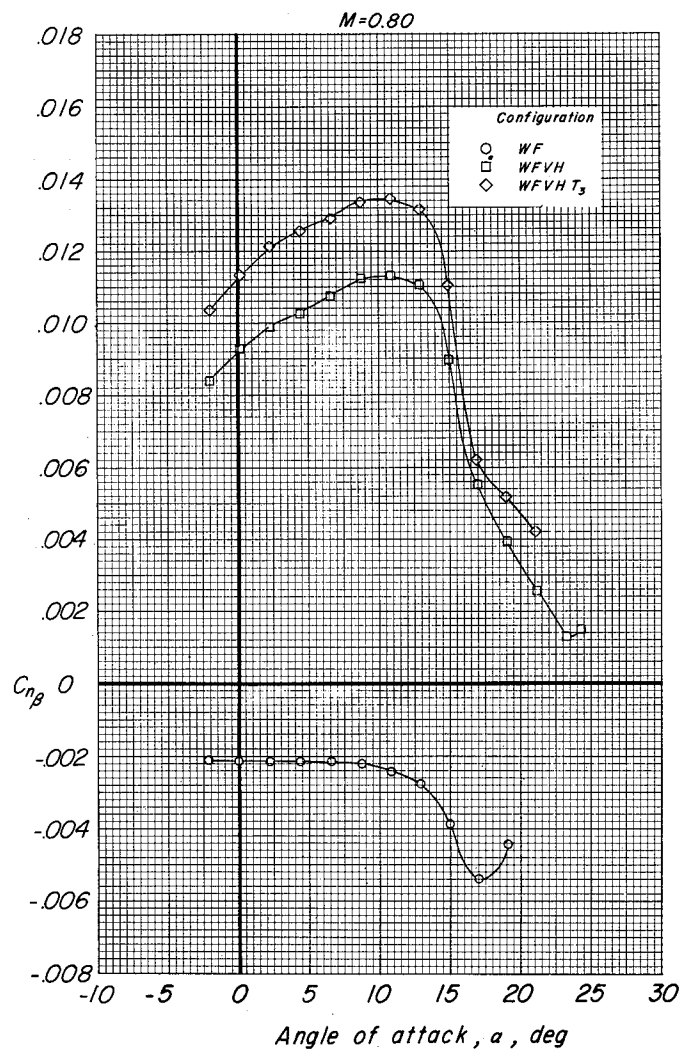

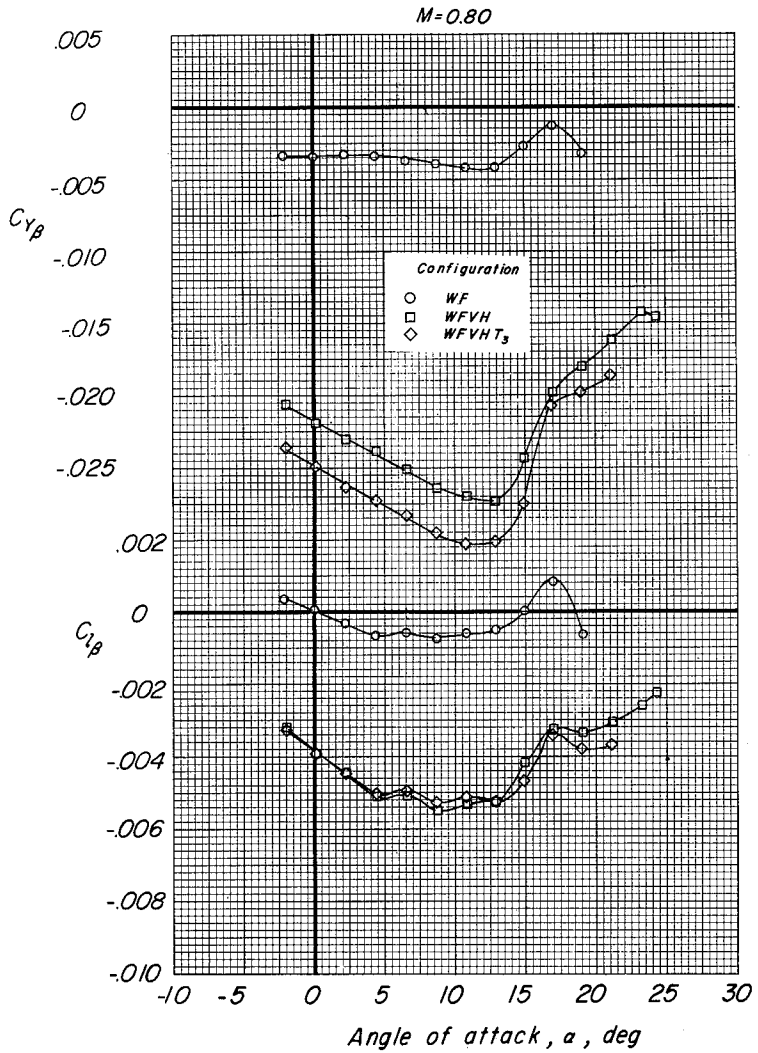

Figure 5.- Continued.

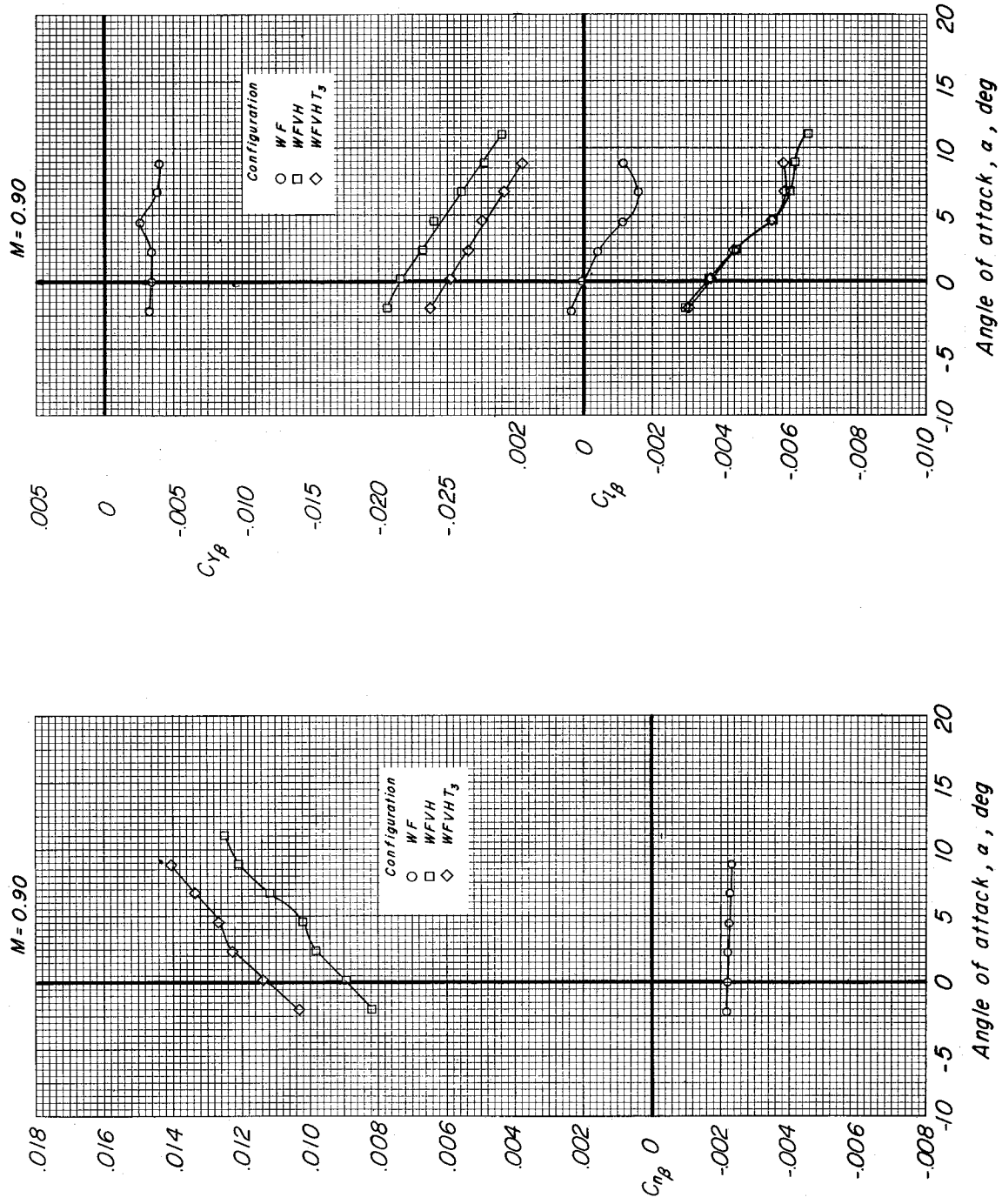

Figure 5.- Continued.

Figure 5.- Concluded.

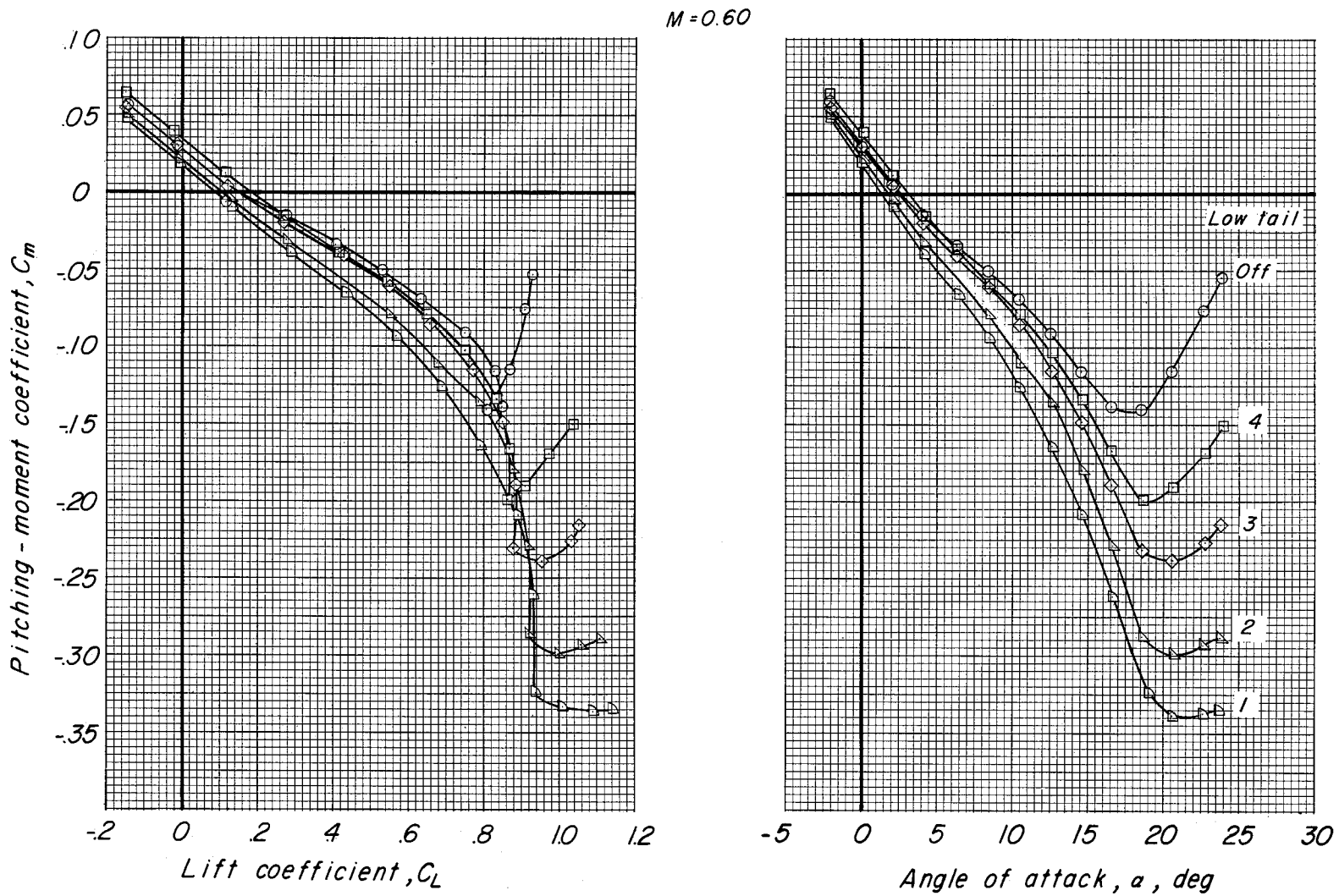

Figure 6.- Pitching-moment characteristics of the model with the moment reference point shifted to give the same low-lift static margin as the basic (high tail only) configuration at M = 0.60. $i_t = -1.4^\circ$.

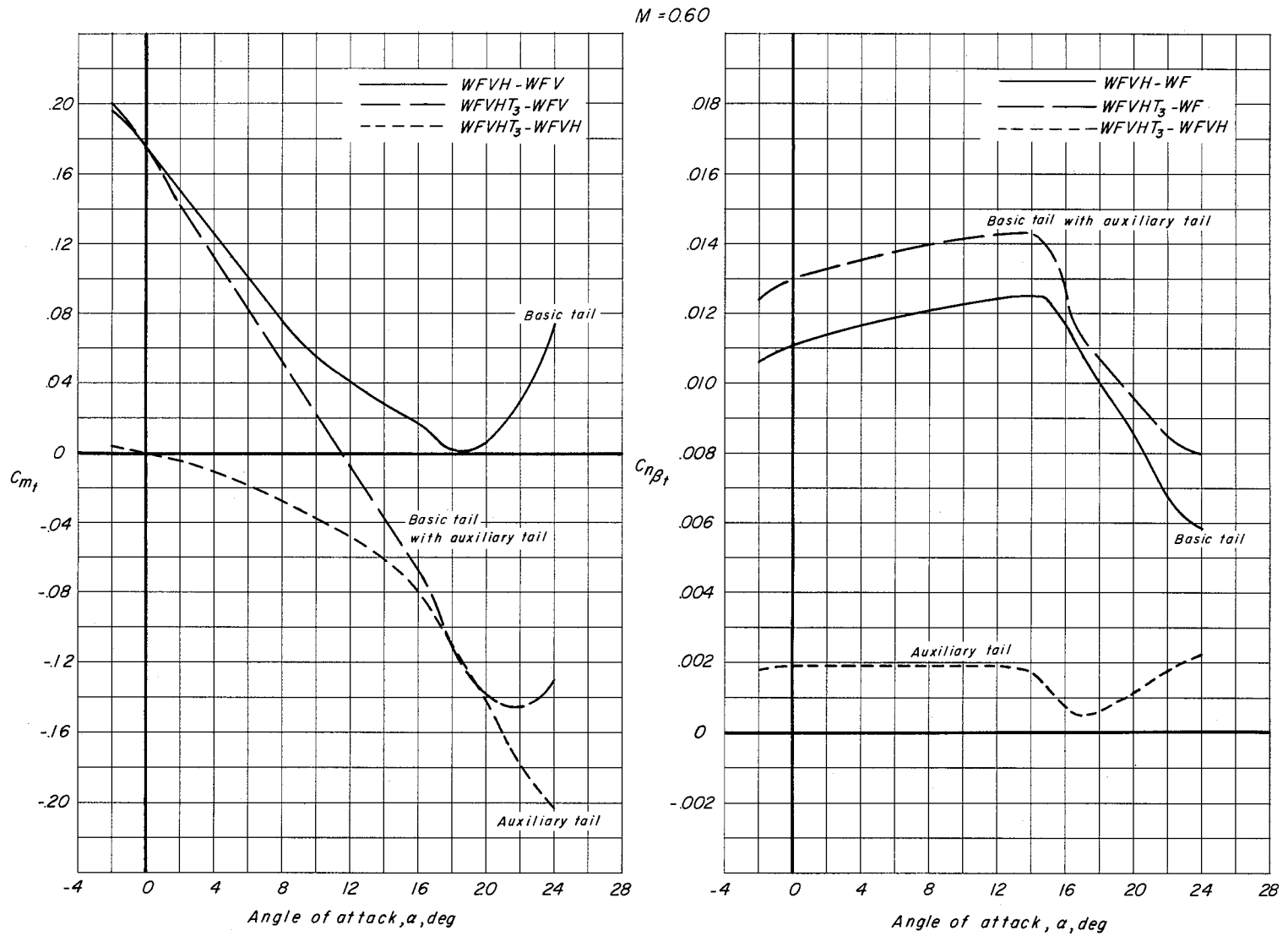

Figure 7.- Contribution of the tail surfaces to pitching moments and directional stability. $i_t = -7.9^\circ$.